rinted in U.S.A.

66-WA/FE-33

an ASME publication

$1.50 PER COPY
75¢ TO ASME MEMBERS

Drag of Blunt Bodies in Polymer Solutions

Effect of High-Molecular-Weight Polymer Additives on the Drag of Falling Cones, Disks, Spheres, and Cylinders in Water

T. G. LANG

H. V. L. PATRICK

Hydrodynamics Group, Research Department
U. S. Naval Ordnance Test Station,
Pasadena, Calif.

Experiments were conducted to determine the effect of high-molecular-weight polymer additives on the drag of cones, disks, spheres, and cylinders. Drop tests were performed in plain water, and in poly(ethylene oxide) (Polyox WSR-301) solutions of 200 and 1000 ppm by weight. Test results showed that sphere drag was reduced by as much as 69 percent, while the drag of the other models were, at most, only slightly reduced by the additives. Dyed-wake photographs of falling spheres showed that the additives could alter markedly the shape of the wake by shifting the point of boundary-layer separation rearward.

Contributed by the Fluids Engineering Division for presentation at the Winter Annual Meeting and Energy Systems Exposition, New York, N. Y., November 27-December 1, 1966, of the American Society of Mechanical Engineers. Manuscript received at ASME Headquarters, August 3, 1966.

Copies will be available until September 1, 1967.

Drag of Blunt Bodies in Polymer Solutions

T. G. LANG

H. V. L. PATRICK

NOMENCLATURE

A = maximum cross-sectional area, sq ft
B = weight of fluid displaced by body, lb
C_D = drag coefficient, $D/A^1/2\rho V^2$, dimensionless
C_{D_o} = measured drag coefficient, dimensionless
d = diameter, ft
D = drag, lb
g = local acceleration due to gravity, 32.13 ft/sec^2
$\bar{h}$ = effective height of body, volume/A, ft
k_1 = virtual mass coefficient, dimensionless
L = length, ft
m_o = mass of fluid displaced by body, B/g, slug
R_d = Reynolds number, Vd/ν, dimensionless
s = distance traveled, ft
t = time, sec
V = speed, fps
V_t = terminal speed, fps
$\dot{V}$ = acceleration, dV/dt, ft/sec^2
W = weight of body, lb
γ = ratio of body density to fluid density, dimensionless
θ = vertex angle of cones, deg
ν = kinematic viscosity, sq ft/sec
ρ = density, slug/cu ft

INTRODUCTION

The addition of certain soluble, high-molecular-weight polymers to water reduces turbulent skin friction by as much as 79 percent (1-5).[1] The drag of a streamlined body is also reduced by the polymer additives, but to a lesser extent (6). As bodies become less streamlined, boundary-layer separation on their aftersections becomes more severe, resulting in greater drag. Cones, disks, spheres, and cylinders are examples of blunt bodies that have extensive regions of separated flow resulting in high drag.

Steel spheres were reported (7) to fall faster in a water solution of guar gum, a high-molecular-weight polymer, than in plain water. A series of drop tests on steel spheres were conducted later (8) in guar-gum solutions varying from 1250 ppm (by weight) to 10,000 ppm and poly(ethylene oxide) (Polyox WSR-301)[2] solutions from 2500 to 15,000 ppm. The spheres ranged in diameter from 0.375 to 1 in. The maximum drag reduction was 28 percent for the 1-in-dia sphere in 5000-ppm guar gum and 7500-ppm Polyox solutions.

To further investigate the effect of polymer additives on the drag of blunt bodies, a series of drop tests were conducted using various cones, stabilized disks, spheres, and cylinders in tap water and in solutions of 200 and 1000 ppm of Polyox. Photographs of the trajectories and of dyed wakes were obtained to aid in the interpretation of the drag data.

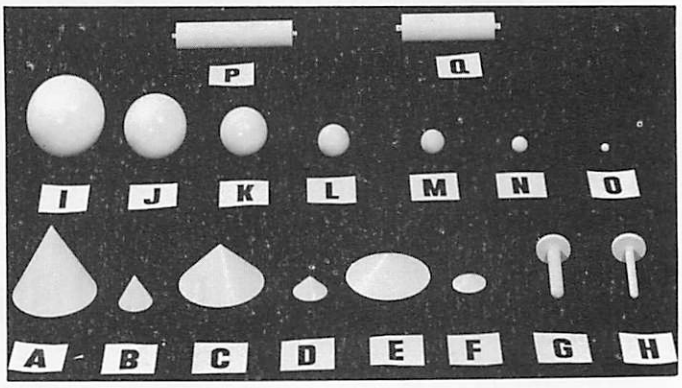

Fig. 1 View of gravity-propelled models

DESCRIPTION OF MODELS AND TEST PROCEDURES

The gravity-propelled models are shown in Fig.1 and their characteristics are listed in Table 1. Models A-F are cones stabilized by lowering the center of gravity by constructing the lower 2/3, measured in height from the vertex upward, of naval brass and the remaining 1/3 of acrylic plastic. Models G and H are 1/8-in-thick acrylic plastic disks with 1.875 in. long, cylindrical naval-brass stabilizers whose diameters are 0.375 and 0.250 in., respectively. Models I-O are stainless-steel spheres. The two cylinders used in the drop tests were designated as models P and Q. Model P is an aluminum cylinder and model Q is an acrylic plastic cylinder with length-to-diameter ratios of 4.55 and 3.41, respectively.

All of the models were coated with white lacquer paint because the data were to be obtained

[1] Numbers in parentheses designate References at the end of the paper.

[2] Union Carbide Chemicals Company, New York, N. Y.

Table 1 Model Characteristics

Model	A	B	C	D	E	F	G	H
Shape	Cone						Disk	
Diameter (in)	2.50	1.00	2.50	1.00	2.50	1.00	1.00	1.00
Cone angle (deg)	60	60	90	90	120	120		

Model	I	J	K	L	M	N	O	P	Q
Shape	Sphere							Cylinder	
Diameter (in)	2.50	2.00	1.50	1.00	0.75	0.50	0.25	1.00	1.00

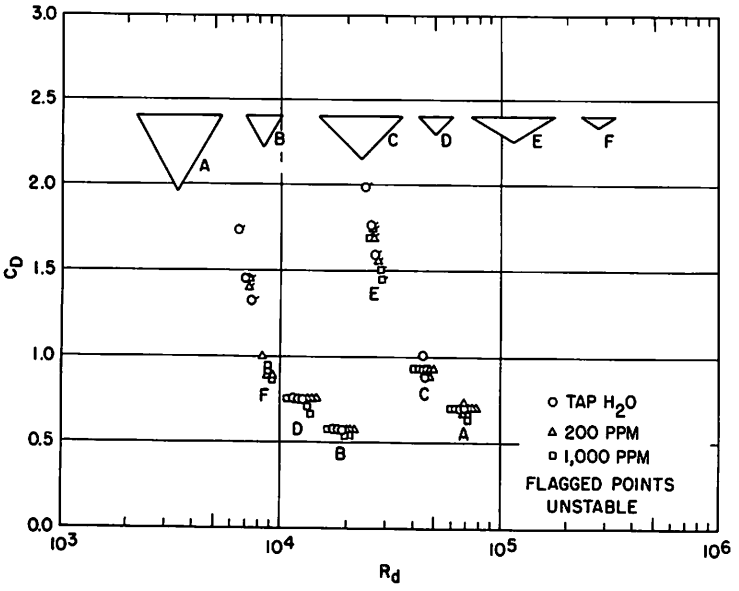

Fig. 2 Effect of Polyox on drag of cones as a function of Reynolds number

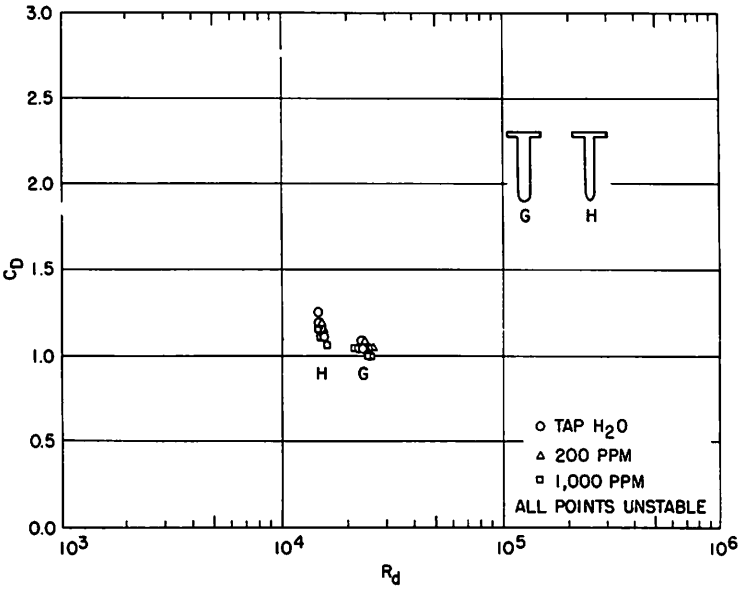

Fig. 3 Effect of Polyox on drag of disks as a function of Reynolds number

photographically and greater contrast was required. The models were then carefully hand rubbed with a fine grade of steel wool to eliminate all visible signs of roughness. Tests consisted of releasing each model by hand in a 7-ft-high tank having an internal cross section of 1 ft by 1 ft and made of clear acrylic plastic. The tank was filled with the test solution to within a few inches of the top. A 2-in-thick pad of polyvinyl-chloride foam (closed cell) was placed at the bottom of the tank to absorb the shock of the falling models. The models were retrieved by a net that normally rested on the pad.

The laboratory was darkened during the tests and the falling models were illuminated by a General Radio Company Strobotac, Model 1531-A, that emitted 1.2 and 3-microsec flashes at a preselected frequency (placed 3 ft to one side of the tank). The falling models were photographed using a 4 x 5 Graphic View camera with a 15-in. Wollensak Graphlex Tele-Optra lens (placed approximately 14 ft in front of the tank). Both the strobotac and the camera were focused near the bottom of the tank. The strobotac was set at the desired frequency and calibrated within ± 1 percent using a counter. The camera lens was opened when each model was released. This procedure resulted in a photographic negative with multiple images. The falling speed of each model was calculated by measuring the distance between images using a precision comparator with an accuracy of plus or minus 1 mil; a photograph of a ruler in the tank provided the scale. The submerged weight of each model was measured on a balance accurate to 0.1 percent.

The drag of spheres can be a function of fluid turbulence, if the model being tested is near the region of transition from laminar to turbulent separation (9), p. 471. Because of this phenomenon, a minimum waiting period of 2 min be-

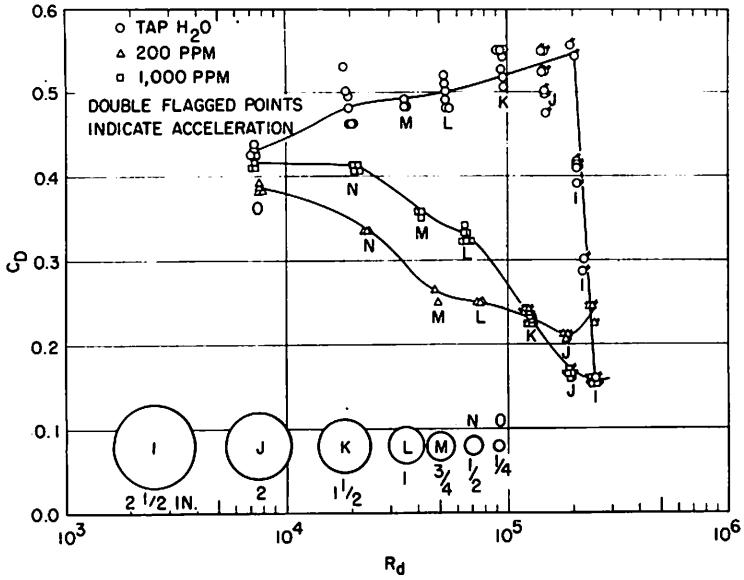

Fig. 4 Effect of Polyox on drag of shperes as a function of Reynolds number

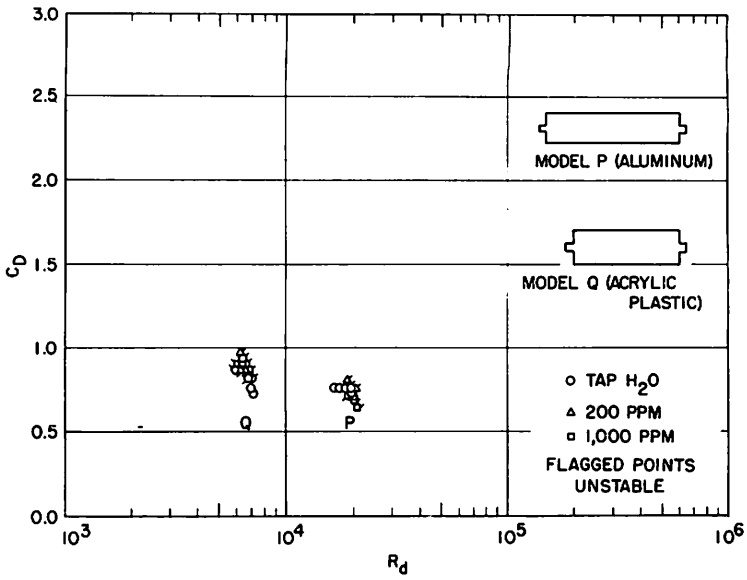

Fig. 5 Effect of Polyox on drag of cylinders as a function of Reynolds number

tween runs was incorporated in the test procedure for spheres I, J, and K.

RESULTS AND ANALYSIS

The drag coefficients of the cones, stabilized disks, spheres, and cylinders are shown in Figs.2-5, respectively, as a function of Reynolds number (based throughout this paper on the properties of plain water). The equations used in data reduction are presented in the Appendix. Reductions in drag up to 69 percent were obtained for the spheres. Little or no drag reduction was measured for the bluff-based objects whose boundary-layer separation point is characteristically fixed and independent of Reynolds number.

The data plots of the stable cones, A, B, C, and D, in Fig.2 indicate a tendency toward reduced drag in the Polyox solutions, although this tendency lies within the data spread. A reduction in the drag of bluff bodies of this type, where the separation point is fixed, is possible if the base pressure is increased. Such a pressure increase in the near wake would cause an enlargement in the near-wake envelope in a manner similar to the enlargement of the cavity envelope produced behind a cone or disk when the cavity pressure is increased. Photographs of the dyed wake of model B in Fig.6 show a slight enlargement of the near wake in the 1000-ppm Polyox solution.

Cones E and F fell much like a falling leaf in plain water. However, cone F was completely stabilized in 1000-ppm solutions and occasionally stabilized in 200-ppm solutions, resulting in an apparent drag reduction of about 38 percent. Although cone E was not stabilized in the Polyox solutions, its apparent drag was reduced by the Polyox.

The drag in plain water of the larger of each pair of geometrically similar cones was about 20 percent greater than that of the smaller cone and was most probably caused by the wall effect. Although wall-effect data on cones are not available, information on spheres falling in tubes (10) indicates an increase in drag of 8 percent for a sphere of the same diameter. The wall effect on a cone would be expected to be greater than 8 percent, since the near wake is larger in diameter than that of an equal-sized sphere.

As in the case of the stable cones, the drag data of the stabilized disks, models G and H, suggest a tendency toward reduced drag in the Polyox solutions, but again, this tendency lies within the data spread. Although both models oscillated in all cases as they fell, model G, the one with the largest stabilizer exhibited the smallest oscillations. Disks without stabilizers are unstable (11) at Reynolds numbers above 180. The drag data for models G and H, shown in Fig.3, are in the vicinity of $C_D = 1.17$ agreeing with data reported in reference (12) for steady state, thin-edged disks. The drag of model G, the disk with the largest stabilizer, is slightly less than that of model H showing that increased stabilizer diameter reduces drag.

In planning the drop tests, calculations showed that steel spheres larger than $1\frac{1}{2}$ in. diameter dropped in plain water would not reach terminal velocity in the 6-ft drop preceding the data-gathering region. Consequently, the drag of the larger spheres was obtained by correcting the data for acceleration to obtain a quasi-steady

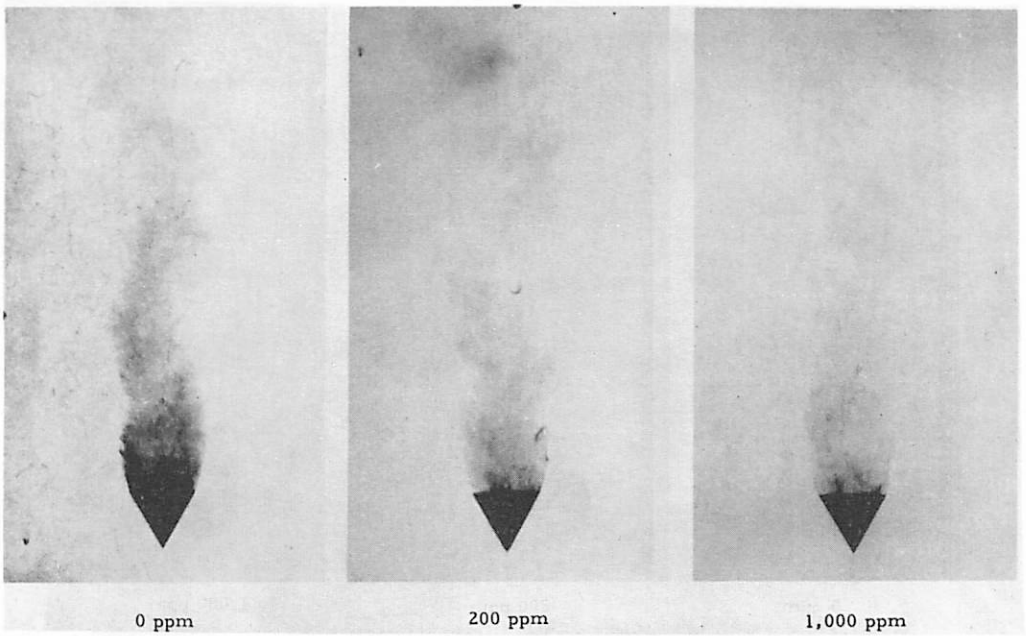

Fig. 6 Dyed-wake photographs of model B (1.00 in. dia and 60-deg cone) in tap water and in solutions of Polyox

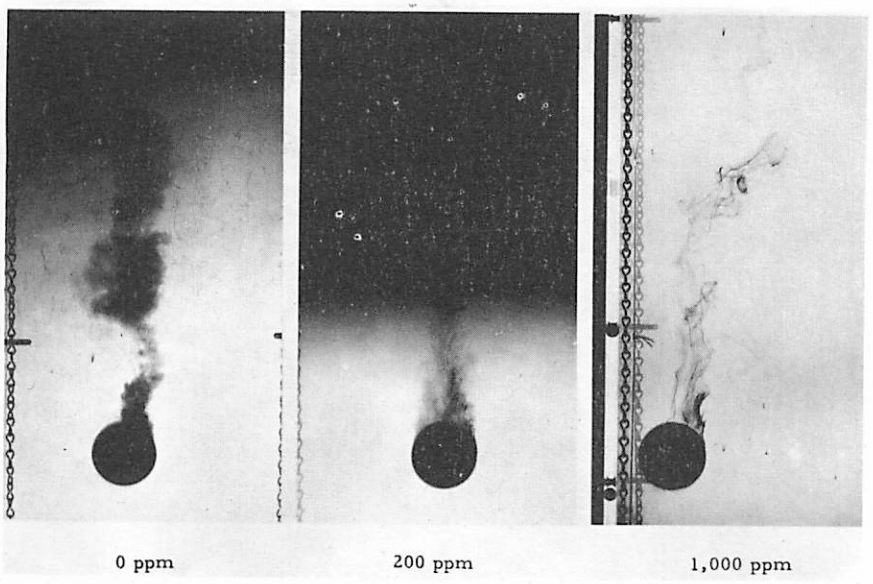

Fig. 7 Dyed-wake photographs of model I (2.500-in-dia sphere) in tap water and in solutions of Polyox

drag coefficient. It was assumed that the acceleration was nearly constant in the relatively short data-gathering region. The equations of motion and data-reduction method are described in the Appendix.

Inspection of Fig. 4 shows that the 200-ppm Polyox solution was more effective than the 1000-ppm solution in reducing sphere drag up to water Reynolds numbers of 0.95×10^5. The drag reductions of spheres in 200 and 1000-ppm solutions of Polyox are listed in Table 2. The maximum drag reduction was 69 percent and occurred for a 2-in. sphere in 1000-ppm Polyox.

It is apparent from the wake photographs of Figs. 7-9 that the separation point was moved rearward on those spheres that exhibited reduced drag. The mechanism that causes the polymer molecules to shift the separation point is not apparent and merits further investigation.

The trajectories of the spheres were nearly vertical, although occasional sudden shifts in direction were noticed. Such shifts were most

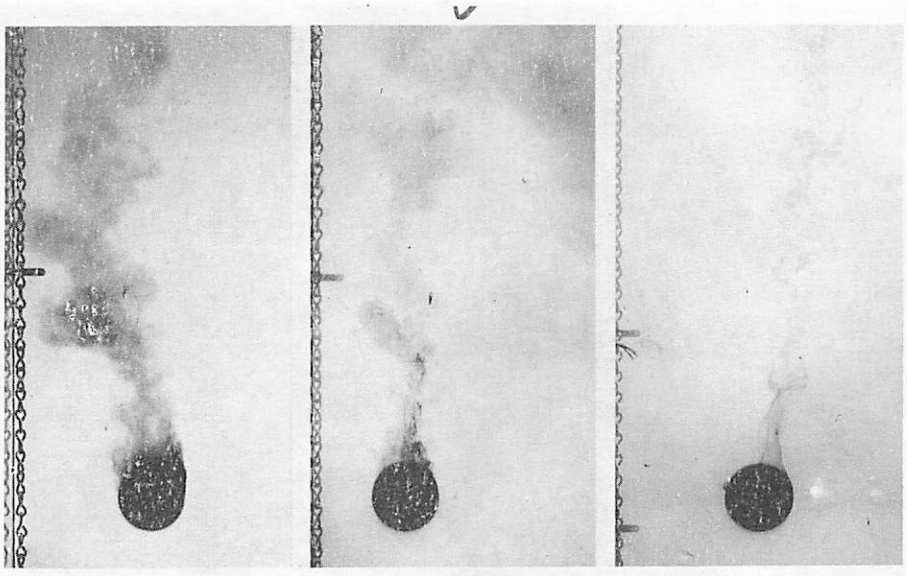

Fig. 8 Dyed-wake photographs of model J (2.00-in-dia sphere) in tap water and in solutions of Polyox

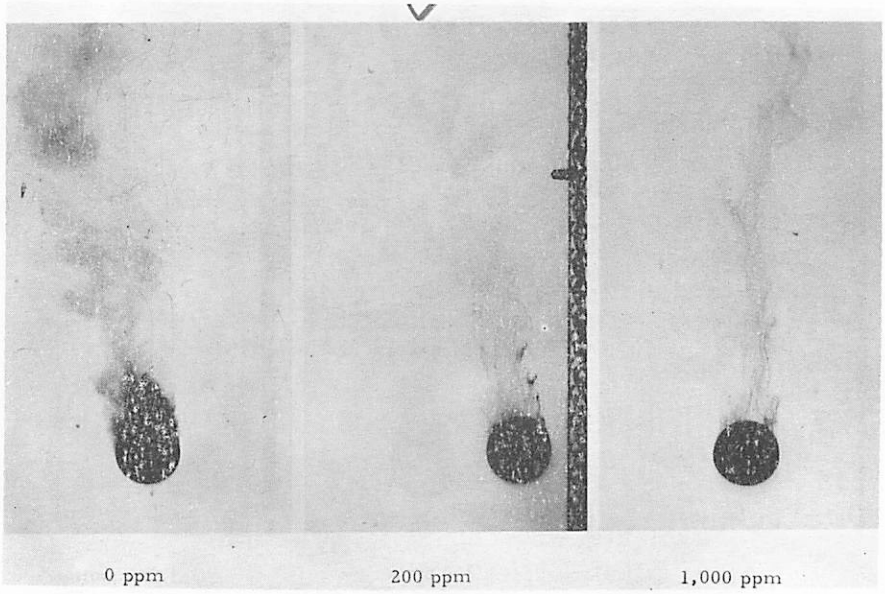

Fig. 9 Dyed-wake photographs of model K (1.50-in-dia sphere) in tap water and in solutions of Polyox

likely due to the release of vorticity illustrated photographically in reference (13), for spheres at Reynolds numbers lower than those being reported. Occasionally, the larger spheres approached, or hit, the tank wall as they neared the bottom; such data were excluded.

The drag data of spheres in plain water compare well with published data (9), p. 16, and (13-14), although considerable variation exists in the published data. The published data show that $C_D \approx 0.40$ in the Reynolds number region of 2×10^3 to 10^4, then increases to 0.50 at $R_d = 2 \times 10^4$ and suddenly decreases to $C_D = 0.08$ or 0.10 at R_d between 1×10^5 and 3×10^5. The sudden decrease in drag is characteristic of transition from laminar boundary-layer separation to turbulent boundary-layer separation. The drag of spheres in Polyox solutions did not follow the typical trend of sphere drag in plain water as a function of Reynolds number. The characteristic sharp decrease in drag, which is due to sudden transition to turbulent separation, did not occur in the Polyox solutions.

The wall effect is possibly significant

Table 2 Drag Reduction of Steel Spheres Falling in 200 and 1000 ppm Solutions of Polyox

Model	I	J	K	L	M	N	O
R_d in plain water, (10^5 units)	2.0	1.4	0.95	0.52	0.34	0.20	0.07
Diameter, (in)	2.50	2.00	1.50	1.00	0.75	0.50	0.25
Drag Reduction in 200 ppm, (%)	-	60	56	50	47	32	11
Drag Reduction in 1000 ppm, (%)	-	69	57	34	28	15	4

only on the two largest spheres. If the Reynolds number was approximately 10^4 the speed of spheres J and I would reduce about 1.5 and 3.5 percent, respectively (10). However, no corrections to the data were made for wall effect since these spheres operated around $R_d = 10^5$ and accurate data on wall effect in this region of R_d were not available. It is likely, however, that the reported drag coefficients of spheres I and J are slightly high.

The drag coefficient of model P (Fig.5), the aluminum cylinder, was slightly reduced by the Polyox, although the data scatter was large. However, the drag of model Q, the lighter acrylic plastic cylinder, was apparently slightly increased by the Polyox solutions, although this increase is within the data scatter. Apparently the moderate reductions in drag in the vicinity of $R_d = 10^4$ exhibited by spheres in Polyox solutions, do not hold for cylinders. The added drag owing to the square ends of the models may have helped mask the effects of the Polyox. The drag coefficients of the few stable drop tests of models P and Q in plain water lie in the region of 0.70 to 0.80 reported (12), p. 3-16 and Fig.28, for cylinders with these length-diameter ratios.

FLOW VISUALIZATION

It has been well established (9), p. 37, that two regimes of fluid flow past spheres exist in the Reynolds number R_d region around 1×10^5 to 3×10^5. The point of boundary-layer separation suddenly moves rearward when the boundary layer of the sphere changes from laminar to turbulent. Rather than separating near the midpoint as in laminar flow, a turbulent boundary layer will remain attached to the sphere for a greater distance before separating, owing to increased mixing of the high-energy outer boundary-layer fluid with the low-energy fluid near the sphere surface. The drag of a sphere reduces if the separation point moves rearward since the near-wake size reduces and the energy loss in the wake eddies reduces. A possible exception is the case of wakes filled with Polyox molecules since it is conceivable that the molecules, or clusters of molecules, can reduce energy loss.

Photographs were taken of the dyed wakes of bodies falling in plain water and polymer solutions to aid in interpreting the drag data. The wakes of sphere models I ($2\frac{1}{2}$ in. dia), J (2 in. dia), and K ($1\frac{1}{2}$ in. dia) and a cone, model B, were photographed. Powdered potassium permanganate crystals were attached to aft end of the models using double-faced adhesive tape. The models were released in such a manner that the tape and crystals would be in the region of the wake thereby causing little disturbance to the flow around the models. Photographs were taken by illuminating the falling models with a high-intensity 3-microsec flash in a darkened laboratory while the camera shutter was open. Test solutions were plain water (0 ppm) and 200 and 1000-ppm solutions of Polyox. The results of these tests on models B, I, J, and K are shown in the photographs of Figs.6-9.

The appearance of the near wakes in Fig.7 shows that the $2\frac{1}{2}$-in-dia sphere (model I) exhibited turbulent-type separation in plain water and the 1000-ppm solution, and near-turbulent-type separation in the 200-ppm solution. This result is consistent with the drag coefficients shown in Fig.4, if the dye photograph in plain water was taken during a drop in which the sphere exhibited turbulent separation. The stringy appearance of the wake in the 1000-ppm solution suggests that turbulent mixing was less intense than in the case of plain water. Although potassium permanganate oxidizes the polymer in solution, it is believed to have negligible effect on the wake shape or wake stringiness since the reaction rate is extremely slow relative to the mixing rate of the eddies in the wake and the falling time of the model. The color of the Polyox solutions changed slowly from the normal purple color of potassium permanganate in plain water, to a yellowish color over a period of approximately 2 hr.

The dyed-wake photographs of the 2-in-dia sphere, model J, are shown in Fig.8. In plain water, separation occurs near the midpoint which is characteristic of laminar separation. The separation point in the 200-ppm solution, however, lies between normal laminar and turbulent separation. In the 1000-ppm solution the separation

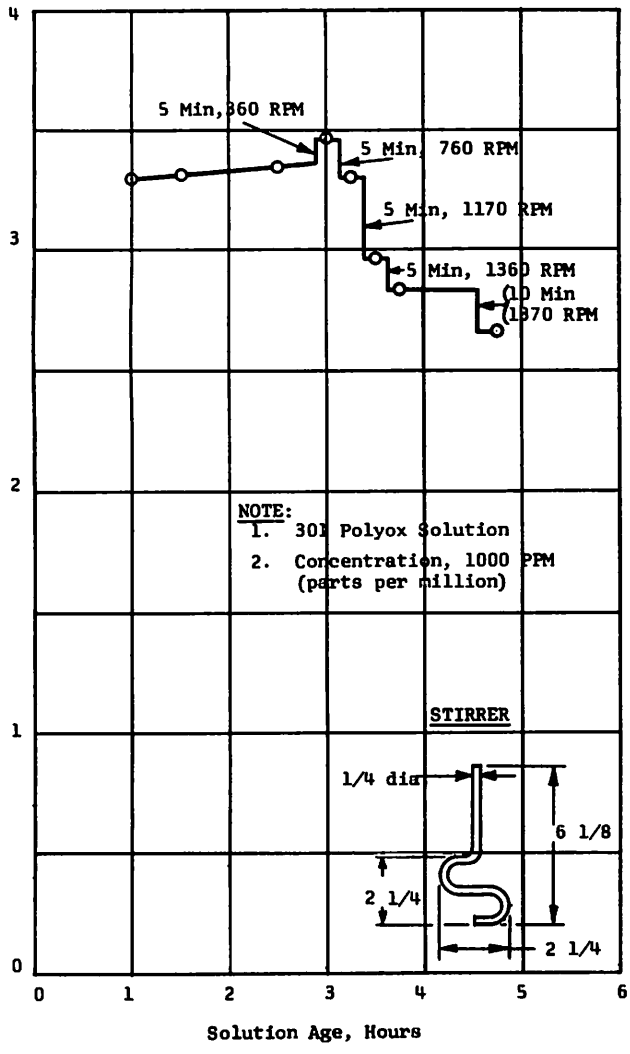

Fig. 10 Effect of mixing rate on the viscosity of a 1000-ppm solution of Polyox

point closely approximates that of normal turbulent separation. The drag coefficient in Fig.4 is seen to reduce as the separation point moves rearward and as the near-wake size reduces.

Shown in Fig.9 are dyed-wake photographs of the 1½-in-dia sphere, model K. As in model J, the separation point shifts rearward with increased Polyox concentration and the near-wake size reduces. The stringiness of the wake in 1000-ppm Polyox is again noted.

Shown in Fig.6 are the dyed-wake photographs of the small 60-deg cone, model B. As expected, there was no change in the point of separation. The increased stringiness of the wake in the Polyox solutions is again noted, suggesting reduced turbulent mixing. The near wake in 1000-ppm Polyox appears to be slightly enlarged, which is expected if the base pressure is increased and the drag reduced as discussed earlier. The drag coefficients shown in Fig.2 appear slightly lower in the 1000-ppm solution than in the 200-ppm solution or in plain water although data scatter is large.

FLUID CHARACTERISTICS

Recent investigations (2) have shown that Polyox in solution, as well as other high-molecular-weight polymers, is susceptible to mechanical degradation; the long chain molecules are broken in regions of high fluid shear. In order to determine whether the mixing speed used in preparing these test solutions was acceptable, a series of tests were performed to determine the effect of mechanical mixing rate on viscosity of a 1000-ppm Polyox solution, assuming that degradation would appear as a reduction in viscosity.

The viscosity was measured by a gravity-flow viscometer consisting of a piece of tubing with a length-to-diameter ratio of 1405 where the id was 0.0338-in. The test solution was siphoned out of a container through the tube and collected in a graduated cylinder. Kinematic viscosity, ν, was evaluated knowing the time taken for a fixed volume to collect in the cylinder. The test solution was hand mixed and then subjected to various degrees of mechanical mixing rate and time period. The results of these tests are shown in Fig.10 where the ratio of viscosity of the solution to that of water at the same temperature is plotted as a function of solution age. A small diagram of the stirrer is shown in the same figure. The various mixing rates and time periods are marked on the curve.

Fig.10 shows that the viscosity increased slightly after resting a short period following hand mixing, and increased considerably after the first mechanical mixing (5 min at 360 rpm). This significant increase in viscosity was felt to be due to completion of hydration of the polymer solution and possibly, better mixing of partially dissolved globules. The viscosity decreased as mixing became more rapid, suggesting that degradation had occurred. It was observed that frothing occurred during mixing that led to reduced viscosity. It was concluded, therefore, that gentle mixing without frothing will probably not cause mechanical degradation of 1000-ppm polymer solutions.

After gentle hand mixing, the solution was observed to have many light-defracting globules distributed throughout, which indicates that the polymer additive was not completely hydrated or mixed. An additional series of tests was performed, therefore, to determine the effect of short-term aging of the solution on drag coefficient. The drag of a 1/2-in-dia sphere, model N, was measured in a 200-wppm Polyox solution that

had been gently hand mixed. Drag data were obtained periodically for a 6-hr period. At approximately 2 hr after solution preparation, the solution was void of any visible light-defracting globules. The drag coefficient was found to be nearly constant throughout the 6-hr testing period, and nearly the same as plotted in Fig.4. It was concluded that incomplete hydration, at the concentration used in testing, does not noticeably affect the drag of spheres.

CONCLUSIONS

The drag of gravity-propelled cones, stabilized disks, spheres, and cylinders was measured in plain water, and in 200 and 1000-ppm solutions of poly(ethylene oxide) (Polyox WSR-301). Photographs of dyed wakes and trajectories were obtained.

The findings are summarized as follows:

1 The maximum drag reduction on spheres was 69 percent for the case of a 2-in-dia steel sphere in a 1000-ppm solution of Polyox at a water Reynolds number of 1.4×10^5.

2 The 200-ppm Polyox solution was more effective in reducing sphere drag than the 1000-ppm solution at water Reynolds numbers up to 0.95×10^5.

3 The concentrated polymer solutions produced a rearward movement of the point of boundary-layer separation on spheres.

4 Polyox produced little or no drag reduction on stable bluff-based bodies; i.e., the cones and disks, whose point of boundary-layer separation is fixed. Also, Polyox additives had little effect on the drag of the cylinders tested.

5 The additives produced an apparent decrease in turbulent mixing in the near wake, as evidenced by photographs of dyed wakes.

6 The additives had a tendency in some cases to stabilize the trajectories of unstable cones resulting in a significant drag reduction.

7 Viscosity tests indicated that no degradation of a Polyox solution occurs if it is mixed gently and frothing avoided.

8 Tests showed no significant effect of solution age on the drag of a 1/2-in. sphere in 200-ppm solution of Polyox.

APPENDIX

MOTION EQUATIONS OF FALLING BODIES

The basic equation of motion for a falling body, including its virtual mass, is

$$(\gamma m_o + k_1 m_o)\dot{V} = W-B - \frac{C_D A \rho V^2}{2}$$

where m_o = water mass displaced by the body, γ = ratio of density of body over density of fluid, k_1 = virtual mass coefficient that represents the effective mass of the fluid carried along by the body, V = falling speed, $\dot{V}$ = acceleration, W = weight of the body in a vacuum, B = weight of fluid displaced by the body, C_D = drag/A $1/2\ \rho V^2$, A = maximum cross-sectional area, and ρ = mass density of the fluid.

Integration of the equation yields

$$V = V_t \tanh(at)$$

where

$$V_t = \text{terminal speed} = \left(\frac{W-B}{\rho A C_D/2}\right)^{1/2}$$

$$a = \frac{\left[(W-B)\rho A C_D/2\right]^{1/2}}{m_o(\gamma + k_1)}$$

and

t = time since release from a stationary position.

Integrating once more to obtain the fall distance s,

$$s = \frac{V_t}{a} \log \cosh(at)$$

The speed will reach $0.99V_t$ when $\tanh(at) = 0.99$. Hence, at = 2.65 and $\log \cosh(at) = 1.96$. The fall distance required for V to reach $0.99V_t$ is

$$s_{0.99} = 1.96 \frac{V_t}{a} = \frac{1.96\, m_o(\gamma + k_1)}{\rho A C_D/2} = \frac{3.92\, \bar{h}(\gamma + k_1)}{C_D}$$

where $\bar{h}$ = volume of body/A = $m_o/\rho A$ = effective height of body. For spheres, $s_{0.99} = 2.62\ d\ (\gamma + k_1)/C_D$, since $\bar{h} = 2d/3$

Accurate values of k_1 for falling spheres are not available. If no wake exists, k_1 is theoretically 0.50 (14); consequently, k_1 for a sphere with turbulent boundary-layer separation, where the wake is small, would approach this value. However, considerable near-wake mass is

Table 3 Acceleration Corrections Used in Data Reduction for Larger Steel Spheres

Model	Solution	Acceleration Correction Factor $\left[1 - \left(\frac{\gamma + k_1}{\gamma - 1}\right)\frac{\dot{V}}{g}\right]$
I, (2.50 in dia)	Plain tap water (laminar separation)	0.808
I	200 ppm Polyox	0.664
I	1000 ppm Polyox	0.467
J, (2.00 in dia)	Plain tap water	0.955
J	200 ppm Polyox	0.651
J	1000 ppm Polyox	0.544
K, (1.50 in dia)	Plain tap water	1.000
K	200 ppm Polyox	0.849
K	1000 ppm Polyox	0.806

carried along by a sphere with laminar boundary-layer separation; such separation normally occurs in water at Reynolds numbers up to about 2×10^5. An estimate of k_1 for a sphere with laminar separation, based on the near-wake volumes in water of model K (Fig.9) is about 1.8.

The value of $s_{0.99}$ for steel spheres with $\gamma = 7.7$, $C_D = 0.50$, and $k_1 = 1.8$ becomes $s_{0.99} = 49.7$ d. Hence, $s_{0.99}$ is 4.1 ft for a 1-in. sphere and 6.2 ft for a $1\frac{1}{2}$-in. sphere, indicating that a correction for acceleration is needed for tests in water of steel spheres over $1\frac{1}{2}$-in. in diameter. If the drag coefficient is reduced, as in the Polyox solutions, k_1 will also reduce, but the net result will be an increase in $s_{0.99}$; consequently, larger acceleration corrections are needed for spheres in Polyox solutions.

The drag coefficient for accelerating bodies is obtained by rewriting the basic motion equation as follows:

$$C_D = \frac{(W-B)-m_o(\gamma + k_1)\dot{V}}{\rho A V^2/2} = C_{D_o}\left[1 - \left(\frac{\gamma + k_1}{\gamma - 1}\right)\frac{\dot{V}}{g}\right]$$

where

$$C_{D_o} = \frac{W - B}{\rho A V^2/2} = \frac{g\, m_o(\gamma - 1)}{\rho A V^2/2}$$

= measured drag coefficient before correction for acceleration

and

$$\left[1 - \left(\frac{\gamma + k_1}{\gamma - 1}\right)\frac{\dot{V}}{g}\right] = \text{acceleration correction factor}$$

In reducing the data, k_1 was assumed to be 0.50 for all spheres in view of the lack of valid experimental data. Also, since considerable scatter existed in the acceleration measurements, an average measured value was used for V in the data reduction of groups of spheres that reached about the same speed in the data-gathering region of the tank. Acceleration was noticeable only for drops of models I and J in plain water and for models I, J, and K in 200 and 1000-ppm Polyox. The magnitudes of the acceleration corrections used in data reduction are listed in Table 3. For model K, the water data may be slightly high since some acceleration may have occurred even though it was not measurable. Also, the water data for models I and and J may be a few percent high in the region of $C_D = 0.50$ since $k_1 = 0.50$ was used in correcting for acceleration rather than the higher estimated value of $k_1 = 1.80$. If valid measurements of k_1 are obtained in the future, these data can be modified accordingly.

REFERENCES

1 A. G. Fabula, "The Toms Phenomenon in the Turbulent Flow of Very Dilute Polymer Solutions," Proceedings of the Fourth International

Congress on Rheology, part 3, Interscience Publishers, New York, N. Y., 1965, pp. 455-479.

2 J. W. Hoyt and A. G. Fabula, "The Effect of Additives on Fluid Friction," NAVWEPS Report 8636, NOTS TP 3670, U. S. Naval Ordnance Test Station (NOTS), China Lake, Calif., December 1964.

3 H. R. Crawford and G. T. Pruitt, "Rheology and Drag Reduction of Some Dilute Polymer Solutions," Final Report, Contract No. N60530-6899 (NOTS), Westco Research, Dallas, Tex., July 1962.

4 J. F. Ripken and M. Pilch, "Non-Newtonian Pipe Friction Studies with Various Dilute Polymer Water Solutions," Project Report No. 71, St. Anthony Falls Hydraulic Laboratory, University of Minnesota, Minneapolis, Minn., June 1964.

5 H. Shin, "Reduction of Drag in Turbulence by Dilute Polymer Solutions," ScD thesis, Department of Chemical Engineering, Massachusetts Institute of Technology, Cambridge, Mass., May 1965.

6 W. M. Vogel and A. M. Patterson, "An Experimental Investigation of the Effect of Additives Injected Into the Boundary Layer of an Underwater Body," Proceedings of the Fifth Symposium on Naval Hydrodynamics, Bergen, Norway, September 12, 1964, ONR, Washington, D. C., 1966.

7 H. R. Crawford and G. T. Pruitt, "Drag Reduction of Dilute Polymer Solutions," Symposium on Non-Newtonian Fluid Mechanics, Fifty Sixth Annual Meeting, American Institute of Chemical Engineering, Houston, Tex., December 5, 1963.

8 M. A. Ruszczycky, "Sphere Drop Tests in High-Polymer Solutions," Nature, vol. 206, May 8, 1965, pp. 614-615.

9 H. Schlichting, "Boundary Layer Theory," fourth edition, McGraw-Hill Book Company, Inc., New York, N. Y., 1960.

10 V. Fidleris and R. L. Whitmore, "Experimental Determination of the Wall Effects for Spheres Falling Axially in Cylindrical Vessels," British Journal of Applied Physics, vol. 12, September 1961, pp. 490-494.

11 W. Willmarth, N. E. Hawk, and R. L. Harvey, "Investigations of the Steady and Unsteady Motion of Freely Falling Disks," Arl 63-176, Aerospace Research Laboratories, University of Michigan, Ann Arbor, Mich., October 1963.

12 S. F. Hoerner, "Fluid-Dynamic Drag," Published by the author, 148 Busteed Drive, Midland Park, N. J., 1958, pp. 3-16.

13 R. H. Magarney and C. S. MacLatchy, "Vortices in Sphere Wakes," Canadian Journal of Physics, vol. 43, no. 9, September 1965, pp. 1649-1656.

14 A. F. Zahm, "Flow and Drag Formulas for Simple Quadrics," NACA Report No. 253, 1926, pp. 517-537.